

SAN098-2307J

**Experimental Demonstration of Guiding and Bending of Electromagnetic Waves in  
a Photonic Crystal**

**Shawn-Yu Lin\*, Edmond Chow, Vince Hietala**

**Sandia National Laboratories, P.O. Box 5800, Albuquerque, NM 87185**

**Pierre R. Villeneuve and J.D. Joannopoulos**

**Department of Physics, Massachusetts Institute of Technology, Cambridge, MA  
02139**

**Abstract**

The routing and interconnection of optical signals through narrow channels and around sharp corners is important for large-scale all-optical circuit applications. A recent computational result suggests that photonic crystals may offer a novel way of achieving this goal by providing a mechanism for guiding light that is fundamentally different from traditional index guiding. Waveguiding in a photonic crystal, and near 100% transmission of electromagnetic waves around sharp  $90^\circ$  corners were observed experimentally. Bending radii were made smaller than one wavelength.

\*To whom correspondence should be addressed. E-mail: [slin@sandia.gov](mailto:slin@sandia.gov)

## **DISCLAIMER**

This report was prepared as an account of work sponsored by an agency of the United States Government. Neither the United States Government nor any agency thereof, nor any of their employees, make any warranty, express or implied, or assumes any legal liability or responsibility for the accuracy, completeness, or usefulness of any information, apparatus, product, or process disclosed, or represents that its use would not infringe privately owned rights. Reference herein to any specific commercial product, process, or service by trade name, trademark, manufacturer, or otherwise does not necessarily constitute or imply its endorsement, recommendation, or favoring by the United States Government or any agency thereof. The views and opinions of authors expressed herein do not necessarily state or reflect those of the United States Government or any agency thereof.

## **DISCLAIMER**

**Portions of this document may be illegible in electronic image products. Images are produced from the best available original document.**

The efficient guiding and interconnection of light on a chip is important for telecommunication and optical computing applications [1,2]. Conventional dielectric waveguides can support guided modes along straight lines with high efficiency, yet are restricted by radiation loss to a moderate bending radius [3]. A recent theoretical investigation suggests that photonic crystals hold the key for overcoming this problem. It is predicted that a photonic crystal waveguide can guide light with great efficiency either along a straight path [4] or around a sharp corner [5-7]. It is further suggested that light can be guided in air minimizing guiding loss due to material absorption.

Photonic crystals, also known as photonic band gap (PBG) materials, are artificially engineered dielectric materials that exhibit a frequency regime over which propagation of light is strictly forbidden [8-11]. A linear defect in a photonic crystal can give rise to a band of defect states within the gap and act as a waveguide (see Fig. 1a). Light in the photonic crystal is confined to and guided along the one-dimensional (1D) channel because the gap forbids light from escaping into the bulk crystal. A waveguide bend ( Fig.1b) can then steer light around a sharp  $90^\circ$  corner. A simple scattering theory predicts the existence of reflection nodes where 100% transmission efficiency can be achieved through the bend [5]. We now demonstrate waveguiding of electromagnetic (EM) waves by a PBG line defect and, more importantly, observe near perfect transmission of EM-waves around a sharp corner in a photonic crystal.

The 2D photonic crystal we used to construct straight waveguides and waveguide bends consisted of a square array of circular Alumina rods having a dielectric constant,  $\epsilon$ , of 8.9 and a radius,  $r$ , of  $0.20a$  where  $a$  is the lattice constant of the square array. In our experiment, the lattice constant is chosen to be 1.27mm. For such a 2D photonic crystal, a large photonic band gap exists for light polarized parallel to the rods that extends from a frequency of  $0.32c/a$  (76 GHz) to  $0.44c/a$  (105 GHz).

A line defect is created inside the crystal by removing a row of rods. The line defect introduces an optical mode inside the crystal. Its localization strength depends on the spe-

cific modal frequency; at mid-gap, the guided mode extends less than one-half wavelength into the crystal [12]. The translational symmetry along the line defect allows the guided mode to be described with two quantum numbers: frequency ( $f$ ) and wavevector ( $k$ ). A  $f$ -versus- $k$  dispersion relation uniquely characterizes the propagation of light in the waveguide. Computed results of such a dispersion relation along the high-symmetry crystal direction  $\langle 10 \rangle$  is shown in Fig. 2, along with the extent of the PBG. The dispersion is strongly nonlinear near the cut off at  $k=0$ . It becomes linear at higher frequencies and eventually intercepts the upper branch of the photonic band gap at  $f=0.44c/a$ . The bandwidth,  $\Delta f$ , of the guided mode is very large, and extends over the entire width of the band gap. Had we chosen a lattice constant,  $a$ , of  $0.59\mu\text{m}$  (infrared regime) instead of  $1.27\text{mm}$  (millimeter-wave regime), the band gap would have been centered at  $1.55\mu\text{m}$  and the guided-mode bandwidth,  $\Delta\lambda$ , would have extended over a range of  $430\text{nm}$ .

To test the PBG waveguides, we use a HP8510C mm-wave source unit with a tunable frequency range from 75 to 110 GHz. The electric-field of the emitted electromagnetic wave is polarized parallel to the dielectric rods, and is coupled into the PBG waveguide with two metallic mm-wave waveguides, a transmitter and a receiver, placed next to the entrance and exit of the PBG waveguide, respectively. This scheme is used to optimize coupling into the PBG waveguide. It closely mirrors the set-up used in the computational simulations [5]. In the simulations, a point dipole, acting as a transmitter, was placed at the entrance of the PBG waveguide, and the field amplitude was monitored at a point located inside the guide after the bend (receiver) [5,13]. In the ideal situation, the experimental set-up would allow for complete coupling of light from the transmitter to the PBG waveguide.

The transmission spectrum of a straight PBG waveguide is shown in Fig. 3a. As expected, the PBG waveguide transmits light over a broad range of frequencies, from  $\sim 80$  to  $\sim 105\text{GHz}$ . The measured spectrum displays a strong  $f$  dependence; its peak is close to mid-gap and transmission falls off near the band edges. The  $f$  dependence is attributed to

mode matching efficiency (i.e. modal overlap) between the mode in the metallic waveguide and the one in the PBG waveguide. The best matching occurs near mid-gap where the modes in both the metallic and PBG waveguides have a similar extent. Near the band edges, the guided mode extends more deeply into the crystal, and mode matching becomes poorer. Also, at the low- $f$  band edge, the group velocity of the guided mode is near zero, making signal detection difficult at the output.

Another distinctive feature of the PBG waveguide is the localization of light in air, reducing signal loss due to material absorption. The only loss comes from a slight penetration of light into the photonic crystal, which is estimated to be  $\sim 10\%$  of its modal volume at mid-gap frequencies. Compared to a ridge dielectric waveguide, signal loss is reduced by a factor 10. By measuring and comparing transmission amplitude of guides with different lengths, the guiding loss of a straight waveguide is estimated to be 0.3dB/cm over the entire bandgap regime. PBG waveguides thus provide a natural solution to the self-absorption problem often encountered in planar integration of active lasers with passive waveguides. They are also advantageous over metallic waveguides as metal waveguides undergo severe signal loss at optical wavelengths.

A PBG waveguide bend may be constructed by joining together three pieces of straight guides which are oriented along the  $\langle 10 \rangle$ ,  $\langle 11 \rangle$  and  $\langle 01 \rangle$  directions, respectively. The  $\langle 10 \rangle$  and  $\langle 01 \rangle$  guides serve as input- and output-coupling waveguides. The  $\langle 11 \rangle$  guide acts as an ultra small  $45^\circ$  mirror that bends the light. To test the device, the transmitter and receiver are placed again next to the entrance and exit of the PBG waveguides. The measured spectrum for the waveguide bend is shown in Fig. 3a with solid circles. As expected, the amplitude through the bend is slightly smaller than that of the straight waveguide over the entire frequency range, with two exceptions; at  $f_1 \sim 87\text{GHz}$  and  $f_2 \sim 101\text{GHz}$ , both spectra have equal amplitudes suggesting that zero-loss transmission is observed through a  $90^\circ$  PBG bend. Moreover, the bending radius for this geometry is less than one wavelength which constitutes the smallest radius ever achieved in any dielectric

waveguide with complete transmission efficiency [14].

To obtain the intrinsic transmission efficiency of the PBG bend, the transmission spectrum through the bend is normalized to that of the straight waveguide. The normalized spectrum is shown in Fig. 3b. The PBG bend exhibits near perfect transmission at  $f_1$  and  $f_2$  [15]. The two arrows indicate the expected position of the reflection nodes computed using the simple model presented in Ref.[5], which uses a single input parameter  $L$  that corresponds to the physical length of the PBG waveguide along the  $\langle 11 \rangle$  direction. In the case presented above,  $L$  is equal to  $2.33 \times \sqrt{2}a$ . The solid red line is a polynomial fit of the data. The theoretical bending efficiency is also shown in Fig. 3b. The peaks in Fig. 3b confirm a subtle and important point about PBG waveguides. Indeed, the detection of light at the end of a straight waveguide would not be a sufficient condition, in itself, to confirm PBG guiding. It is the existence of transmission peaks around the sharp bend, along with the specific position of these peaks, that validate the model.

The position of the peaks can be predicted using a 1D scattering theory [5]. The  $\langle 11 \rangle$  bending section is modeled as a scattering center with a channel length  $L$  (Fig.4). Light propagating along the  $\langle 10 \rangle$  direction is scattered by the  $\langle 11 \rangle$  section into the  $\langle 01 \rangle$  direction. We label the wavevectors associated with the  $\langle 10 \rangle$ ,  $\langle 11 \rangle$ , and  $\langle 01 \rangle$  states as  $k_1(f)$ ,  $k_2(f)$ , and  $k_1(f)$ , respectively. The strength of the scattering is determined by the mismatch between  $k_1$  and  $k_2$ . If the mismatch is small (the dispersion  $k(f)$  is close to being isotropic) forward scattering is favored and high transmission efficiency is expected. Complete forward scattering occurs when a resonance inside the bend is established. At such a resonance, light travels freely through the bend with 100% efficiency.

Quantitatively, the reflection coefficient near the transmission peaks is given by:  $R(f) \cong 4 \times \left( \frac{\Delta k}{k} \right)^2 \times (\sin k_2 L)^2$ , where  $\Delta k = (k_1 - k_2)/2$  is the wavevector mismatch and  $k = (k_1 + k_2)/2$  is the average wavevector. Resonance occurs when:  $\sin(k_2(f) \times L) = 0$ . The position of the transmission peaks can readily be obtained by computing the dispersion relation  $k_2(f)$  and by determining the length of the  $\langle 11 \rangle$  waveguide section. For the

bending geometry shown in the inset of Fig. 3b, we find  $f_1=87.5\text{GHz}$  and  $f_2=101\text{GHz}$ . To further test the 1D scattering theory, measurements were carried out for different bending geometries with  $L=1.33 \times \sqrt{2}a$  and  $L=3.33 \times \sqrt{2}a$ . The measured and computed peaks are given in Table 1. The agreement between experiment and theory is excellent confirming the validity of the 1D model, hence confirming the existence of guided modes in the photonic crystal.

The 1D model also predicts high transmission efficiency in PBG waveguides with zero radius of curvature. A schematic of the bending geometry is shown in Fig. 3c along with the experimental data. As predicted, the transmission spectrum does not display a series of peaks, yet shows an overall transmission efficiency larger than 80%. This high transmission efficiency is to be compared with ~30% transmission efficiency in similar high-index dielectric waveguides [5].



### References and Notes

1. See, for example, "Applied Photonics", by Chai Yeh, Academic Press, San Diego, California, USA in 1994.
2. C. Wu, Science News, vol. 150, p.309 (1996); Gary Taubes, Science, vol. 278, p.1709-1710(1997).
3. E.A.J. Marcatili, Bell Syst. Tech. 48, 2103 (1969).
4. J. D. Joannopoulos, R. D. Meade, and J. N. Winn, "Photonic Crystals" (Princeton, New York, 1995).
5. A. Mekis, J.C. Chen, I. Kurland, S. Fan, P.R. Villeneuve and J.D. Joannopoulos, Phys. Rev. Lett. 77, 3787 (1996).
6. M.M. Sigalas, R. Biswas, K.M. Ho, C.M. Soukoulis and D.D. Crouch, Proceedings of the 14th Annual Review of Progress in Applied Computational Electromagnetics, p.144 Monterey, CA, March 16-20(1998).
7. J.D. Joannopoulos, P.R. Villeneuve, and S. Fan, Nature, 386, 143 (1997).
8. E. Yablonovitch and T.J. Gmitter, Phys. Rev. Lett. 63, 1950 (1989).
9. K.M. Ho, C.T. Chan, and C.M. Soukoulis, Phys. Rev. Lett. 65, 3152 (1990).
10. K.M. Leung and Y.F. Liu, Phys. Rev. Lett. 65, 2646 (1990).
11. H.S. Sozuer, J.W. Haus, J. Opt. Sc. Ame. B 10, 296 (1993).
12. S.Y. Lin, G. Arjavalingam, Optics Lett. 18, 1666 (1993).
13. J.C. Chen and K. Li, Microwave Opt. Tech. Lett. 10, 319 (1995).
14. To the best of our knowledge, even for a metallic mm-wave 90° waveguide bend, the best commercially available one has a bending radii of 4-5 $\lambda$ .
15. Our measurement is accurate to about  $\pm 5\%$  due mainly to an amplitude oscillation caused by resonance between the input- and output-end of the PBG-guide. Also, the absolute bending efficiency is slightly lower,  $\sim 3\%$ , since the  $\langle 10 \rangle$  and  $\langle 01 \rangle$  sections of the bend would contribute to a small guiding loss.
16. The work at Sandia National Laboratories is supported through DOE under contract

no. DE-AC04-94AL85000. Sandia is a multiprogram laboratory operated by Sandia Corporation, a Lockheed Martin Company, for the United States Department of Energy. The work at MIT is supported in part by the MRSEC program of the NSF under award no. DMR-9400334.

### Figure Captions

Fig. 1 (a) Schematic diagram of a photonic-crystal straight waveguide. (b) Schematic diagram of a photonic-crystal waveguide bend. The green rods are made of dielectric material. The red arrows indicate the direction of light flow.

Fig.2 Dispersion relation of the guided modes along a line defect in the  $\langle 10 \rangle$  direction. Light propagates along the PBG channel according to the specific  $k$ -vs- $f$  relation.

Fig.3a Transmission spectra for a straight waveguide (blue squares) and for a waveguide bend (red circles) in a 2D photonic crystal. The amplitudes of the two curves are equal at frequencies  $f_1 \sim 87\text{GHz}$  and  $f_2 \sim 101\text{GHz}$ , suggesting zero-loss transmission through the sharp  $90^\circ$  corner.

Fig.3b Bending efficiency as a function of frequency. The solid circles correspond to experimental data; the open circles are obtained from theory. Near perfect bending efficiency is observed around  $87\text{GHz}$  and  $101\text{GHz}$ . The black arrows indicate the position of the predicted peaks. The PBG bending geometry is shown in the inset.

Fig.3c Bending efficiency of a PBG waveguide bend with zero radius of curvature. High transmission exceeding  $80\%$  is observed. The open and solid circles correspond to theoretical and experimental data, respectively.

Fig.4 Schematic diagram of the 1D scattering process. The  $\langle 11 \rangle$  bending section is modeled as a scattering center. Scattering arises from the wavevector mismatch between the  $\langle 10 \rangle$  and  $\langle 11 \rangle$  sections. Complete forward scattering occurs when light propagating along the  $\langle 10 \rangle$  direction is in resonance with the  $\langle 11 \rangle$  bending section.

**Table Captions**

Table 1 Experimentally observed and computationally predicted transmission peaks for three different bending lengths  $L$ .

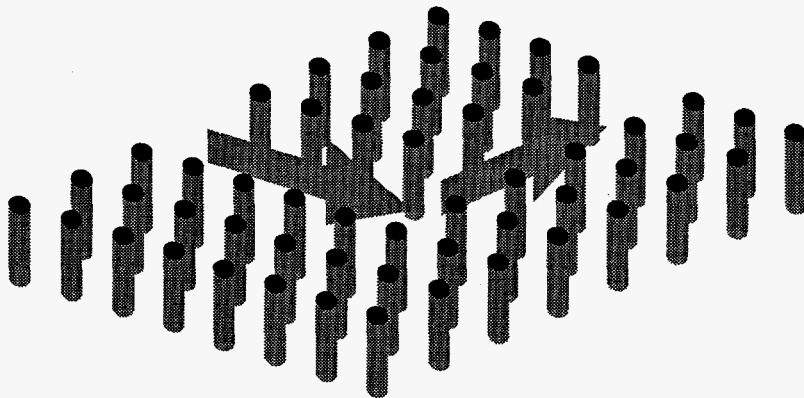
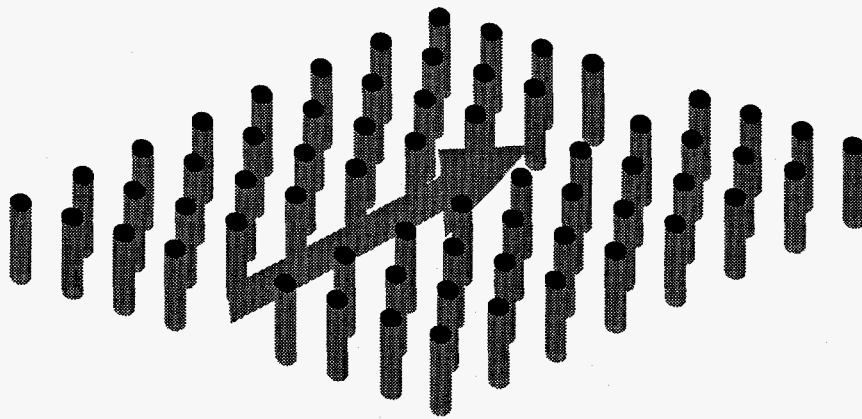


Fig.1(a),(b)

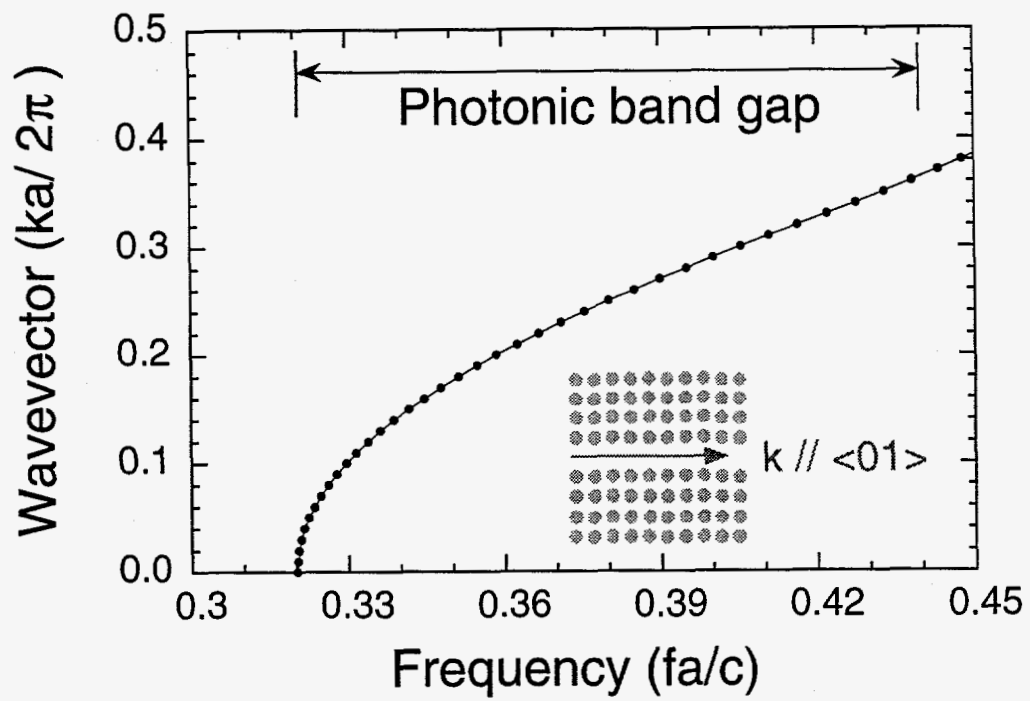
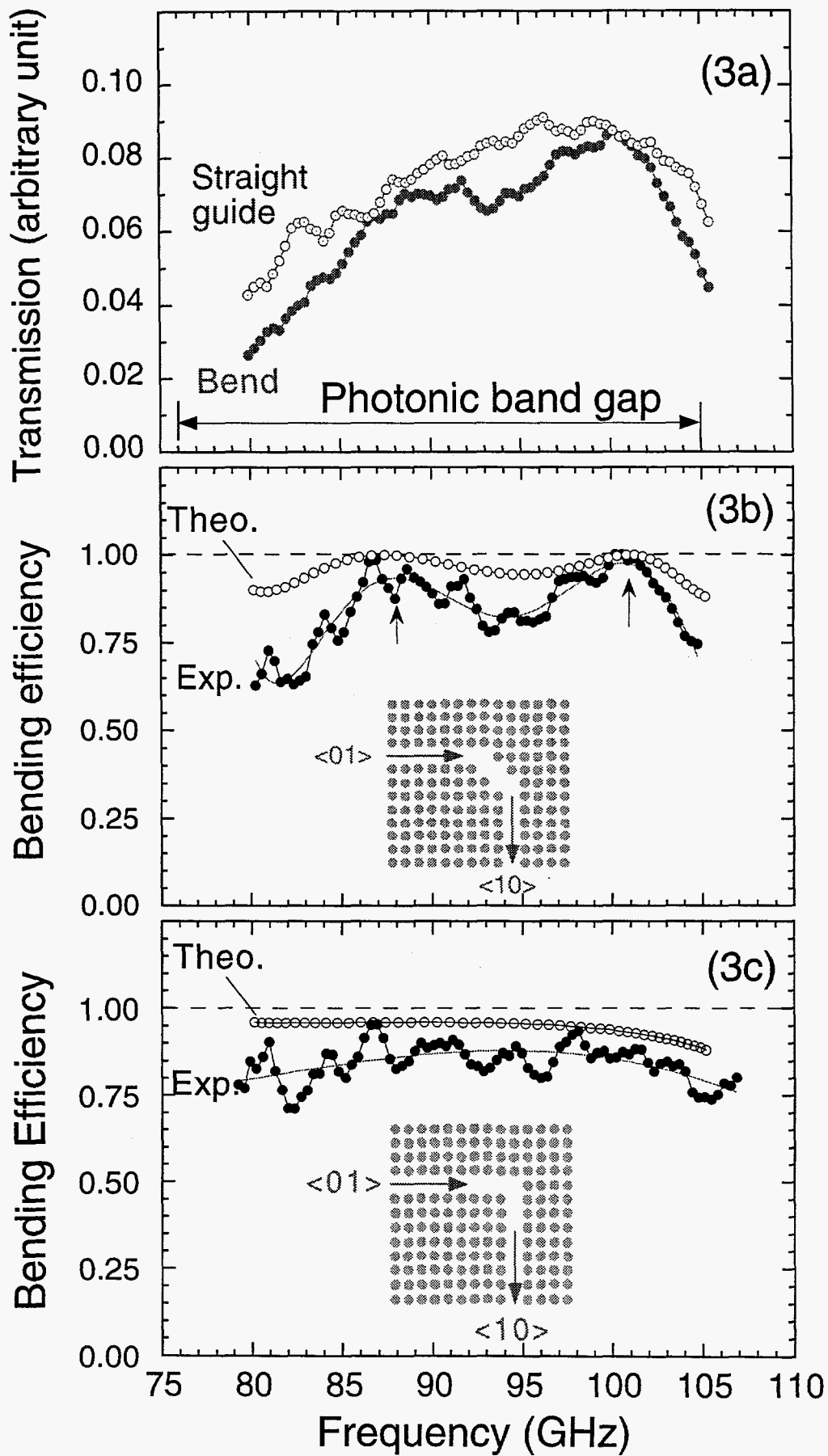


Fig.2



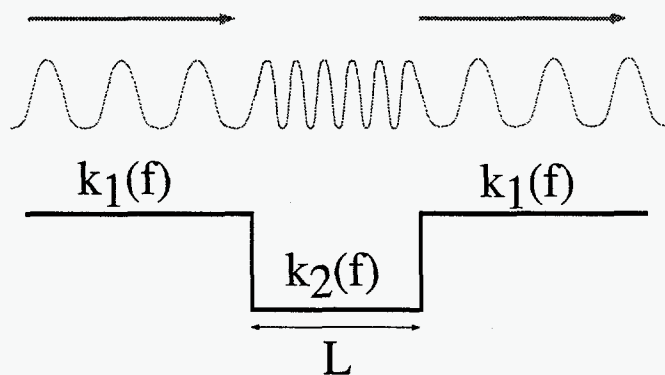


Fig.4

L	$f_1(\text{GHz})$		$f_2(\text{GHz})$	
	Theory	Exp.	Theory	Exp.
1.33	84.0	$86 \pm 3$	105	$102 \pm 3$
2.33	87.5	$88 \pm 3$	101	$101 \pm 3$
3.33	89.0	$88 \pm 3$	99.0	$99 \pm 3$

Table-I